

Isoscaling and the symmetry energy in spectator fragmentation

W. TRAUTMANN¹⁾, A.S. BOTVINA^{1,2)}, J. BRZYCHCZYK³⁾,
A. LE FÈVRE¹⁾, P. PAWŁOWSKI⁴⁾, C. SFIENTI^{1,5)}
AND THE ALADIN AND INDRA COLLABORATIONS

- ¹⁾ Gesellschaft für Schwerionenforschung, D-64291 Darmstadt, Germany
²⁾ Institute for Nuclear Research, 117312 Moscow, Russia
³⁾ M. Smoluchowski Institute of Physics, PL-30059 Kraków, Poland
⁴⁾ H. Niewodniczański Institute, PL-31342 Kraków, Poland
⁵⁾ Dipartimento di Fisica and LNS-INFN, I-95126 Catania, Italy

Abstract

Isoscaling and its relation to the symmetry energy in the fragmentation of excited residues produced at relativistic energies were studied in two experiments conducted at the GSI laboratory. The INDRA multidetector has been used to detect and identify light particles and fragments with $Z \leq 5$ in collisions of ^{12}C on $^{112,124}\text{Sn}$ at incident energies of 300 and 600 MeV per nucleon. Isoscaling is observed, and the deduced parameters decrease with increasing centrality. Symmetry term coefficients, deduced within the statistical description of isotopic scaling, are near $\gamma = 25$ MeV for peripheral and $\gamma < 15$ MeV for central collisions.

In a very recent experiment with the ALADIN spectrometer, the possibility of using secondary beams for reaction studies at relativistic energies has been explored. Beams of ^{107}Sn , ^{124}Sn , ^{124}La , and ^{197}Au were used to investigate the mass and isospin dependence of projectile fragmentation at 600 MeV per nucleon. The decrease of the isoscaling parameters is confirmed and extended over the full fragmentation regime covered in these reactions.

1 Introduction

The symmetry energy and its density dependence have received increasing attention in recent years because of their importance for nuclear structure and for astrophysics. Supernova simulations or neutron star models require inputs for the nuclear equation of state at extreme values of density and asymmetry [1, 2]. The strength of the symmetry term at about normal density is quite well known from the masses of finite nuclei but its density dependence is experimentally very poorly constrained. Theoretical predictions are quite consistent for low-density nuclear matter [3] but diverge considerably at higher density where they are important for astrophysical phenomena as, e.g., the cooling of neutron stars [4]. Nuclear reactions offer the possibility to investigate nuclear matter at densities other than normal nuclear density, and an active search for observables suited to probe the strength of the symmetry term in reaction experiments is presently underway [4, 5, 6].

Multifragmentation is generally considered a low-density phenomenon. However, the short-range nature of the nuclear forces causes a clustering in nuclear systems that have expanded as a result of an initial compression or heating in the course of a violent nuclear collision. Nuclear matter is not homogeneous under such conditions and the strength of the symmetry term is thus not easy to predict. In statistical multifragmentation models, it is assumed that normal-density fragments are distributed within an expanded volume. The density is only low on average, and standard liquid-drop parameters are used to describe the nascent fragments including their isotopic degrees of freedom. In the Copenhagen version of this model (SMM), the symmetry energy term $E_{\text{sym}} = \gamma(A - 2Z)^2/A$ is used with coefficients in the range $\gamma = 23$ to 25 MeV [7, 8].

The knowledge of the strength of the symmetry term under such conditions is of particular interest because the subnuclear densities and the temperatures reached at the freeze-out in fragmentation reactions overlap with those expected for the explosion stages of core-collapse supernovae [9]. This similarity permits laboratory studies of the properties of nuclear matter in the hot environment similar to the astrophysical situation. Nuclear matter in equilibrium at low density is expected to consist of nuclei with a wide range of masses and with properties that dependent strongly on the global parameters of temperature, density, proton fraction and, in particular, also on the strength of the symmetry term under these conditions (Fig. 1).

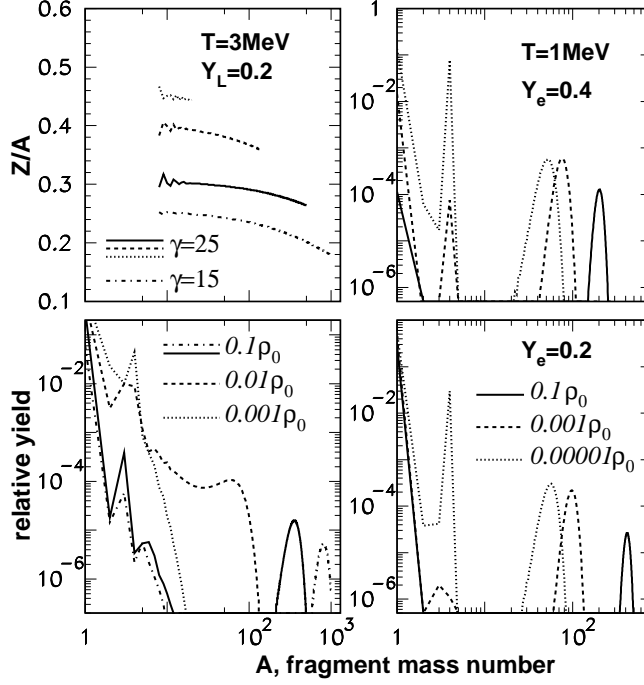


Figure 1: Mean charge-to-mass ratios (left top panel), and mass distributions of hot primary fragments (other panels) calculated with the SMM generalized for supernova conditions. Results are shown for $T = 3$ MeV and fixed lepton fraction $Y_L = 0.2$ (left panels) and $T = 1$ MeV and fixed electron fractions $Y_e = 0.4$ and 0.2 (right panels). Baryon densities are chosen as indicated. The dash-dotted lines represent calculations for density $0.1 \rho_0$ and a reduced symmetry term coefficient $\gamma = 15$ MeV (from [9]).

2 Statistical description of isoscaling

Isotopic scaling, also termed isoscaling, has been shown to be a phenomenon common to many different types of heavy ion reactions [8, 10, 11, 12]. It is observed by comparing product yields from otherwise identical reactions with isotopically different projectiles or targets, and it is constituted by an exponential dependence of the yield ratios $R_{21}(N, Z)$ measured for the two reactions on the neutron number N and proton number Z of the produced fragments. The scaling expression

$$R_{21}(N, Z) = Y_2(N, Z)/Y_1(N, Z) = C \cdot \exp(\alpha \cdot N + \beta \cdot Z) \quad (1)$$

describes rather well the measured ratios for a wide range of complex particles and light fragments [13].

In the grand-canonical approximation, assuming that the temperature T is about the same, the scaling parameters α and β are proportional to the differences of the neutron and proton chemical potentials for the two systems, $\alpha = \Delta\mu_n/T$ and $\beta = \Delta\mu_p/T$. Of particular interest is the proportionality of the scaling parameters with the symmetry energy term. It has been obtained from the statistical interpretation of isoscaling within the SMM [8] and Expanding-Emitting-Source Model [13] and confirmed by an analysis of reaction dynamics [14]. The relation is

$$\Delta\mu_n = \mu_n^1 - \mu_n^2 \approx -4\gamma\left(\frac{Z_1^2}{A_1^2} - \frac{Z_2^2}{A_2^2}\right) = -4\gamma\Delta(Z^2/A^2) \quad (2)$$

where Z_1, A_1 and Z_2, A_2 are the charges and mass numbers of the two systems. The difference of the chemical potential depends essentially only on the coefficient γ of the symmetry term and on the isotopic compositions.

There is a simple physical explanation within the SMM why isoscaling should appear in finite systems. Charge distributions of fragments with fixed mass numbers A , as well as mass distributions for fixed Z , are approximately Gaussian with average values and variances which are connected with the temperature, the symmetry coefficient, and other parameters. The mean values depend on the total mass and charge of the systems, e.g. via the chemical potentials in the grand canonical approximation, while the variances depend mainly on the physical conditions reached, the temperature, the density and possibly other variables. For example, the charge variance $\sigma_Z \approx \sqrt{(AT/8\gamma)}$ obtained for fragments with a given mass number A in Ref. [15] is only a function of the temperature and of the symmetry term coefficient since the Coulomb contribution is very small.

The above relation opens the possibility for an experimental program for studying the evolution of the role of the symmetry term for the fragment formation as a function of the conditions of the experiment. Besides the isoscaling coefficient, the required inputs are the temperatures at breakup and the difference of the neutron-to-proton ratios N/Z of the two systems. An encouraging result was obtained when this method was first applied to the data of light-ion (p, d, α) induced reactions at relativistic energies of up to 15 GeV [8]. The obtained value had about standard magnitude $\gamma \approx 23$ MeV. This is not unexpected in this case because the data were inclusive. These reactions proceed mainly through heavy-residue formation, and the mean multiplicities of intermediate-mass fragments are correspondingly small [16].

3 ^{12}C on $^{112,124}\text{Sn}$ with INDRA@GSI

Multifragmentation becomes a dominant channel in reactions of heavier projectiles or targets at relativistic energies. For the ^{12}C on $^{112,124}\text{Sn}$ reactions, studied with the INDRA multidetector [18] in experiments performed at the GSI, maximum fragment production occurs at central impact parameters, according to the systematics [19]. The measurements were performed with enriched targets of ^{112}Sn (98.9%) and ^{124}Sn (99.9%). Reaction products with $Z \leq 5$ were detected and isotopically identified with high resolution by using the calibration telescopes of INDRA which are positioned at polar angles $45^\circ \leq \theta_{\text{lab}} \leq 176^\circ$ [20].

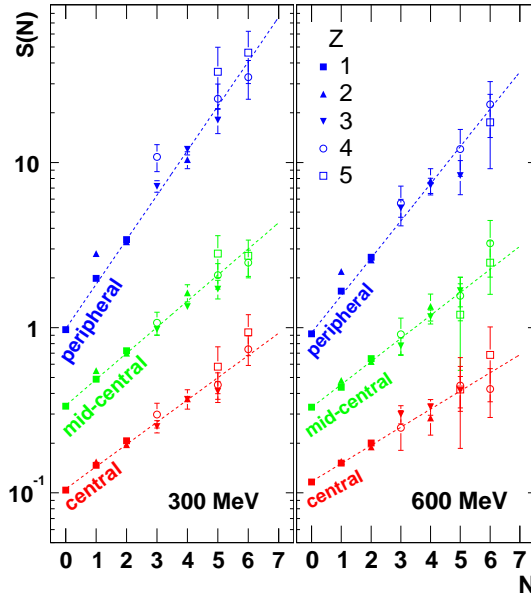


Figure 2: Scaled isotopic ratios $S(N)$ for $^{12}\text{C} + ^{112,124}\text{Sn}$ at $E/A = 300$ MeV (left panel) and 600 MeV (right panel) for three intervals of reduced impact parameter with "central" indicating $b/b_{\text{max}} \leq 0.4$ and with offset factors of multiples of three. The dashed lines are the results of exponential fits according to Eq. (1). Only statistical errors are displayed (from [20]).

The ratios of the energy-integrated fragment yields measured for the two reactions and integrated over energy and angle obey the laws of isoscaling. This is illustrated in Fig. 2 for both incident energies and for three impact parameter bins, selected on the basis of the charged-particle multiplicity measured with the full detector. The fitted dependence on Z has been used

to scale the ratios so as to obtain a single branch for each data set. The resulting slopes of the scaled ratios as a function of the neutron number N change considerably with impact parameter. The obtained fit parameters extend from $\alpha = 0.61$ to values as low as $\alpha = 0.25$ for the most central event group at 600 MeV per nucleon.

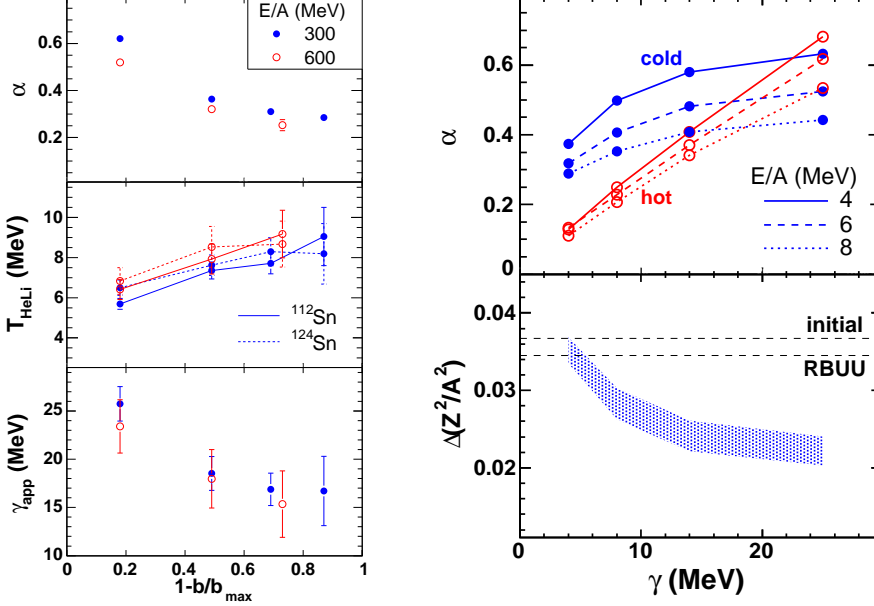


Figure 3: The left panels show the isoscaling coefficient α (top), the double-isotope temperatures T_{HeLi} (middle) and the resulting γ_{app} (bottom) for the ^{12}C on $^{112,124}\text{Sn}$ reactions at $E/A = 300$ MeV (full symbols) and 600 MeV (open symbols) as a function of the centrality parameter $1 - b/b_{\max}$.

The top right panel shows the isoscaling coefficient α for hot (open circles) and cold fragments (dots) as a function of the symmetry term coefficient γ as predicted by the Markov-chain calculations for $^{112,124}\text{Sn}$. The shaded area in the bottom right panel shows the region in the $\Delta(Z^2/A^2)$ -versus- γ plane that is consistent with the measured value $\alpha = 0.29$ for central collisions and with the Markov-chain predictions for cold fragments. The dashed lines indicate the $\Delta(Z^2/A^2) = 0.0367$ of $^{112,124}\text{Sn}$ and the RBUU prediction (from [20]).

With temperature estimates obtained from the yields of $^3,^4\text{He}$ and $^6,^7\text{Li}$ isotopes, the values for an apparent symmetry term γ_{app} , i.e. before sequential decay corrections, were obtained according to Eq. 2. For peripheral collisions, they are close to the normal-density value $\gamma \approx 23$ MeV but drop to lower values at the more central impact parameters (Fig. 3, bottom left). The effects of sequential decay for the symmetry term were calculated within the microcanonical Markov-chain version of the Statistical Multifragmenta-

tion Model [17] for excitation energies of 4, 6, and 8 MeV per nucleon and for $4 \text{ MeV} \leq \gamma \leq 25 \text{ MeV}$. The isoscaling coefficient α was determined from the calculated fragment yields before (hot fragments) and after (cold fragments) the sequential decay part of the code for which a standard value $\gamma = 25 \text{ MeV}$ was used.

The hot fragments exhibit the linear relation of α with γ as expected (Fig. 3, top right). For γ smaller than 25 MeV, the sequential decay causes a narrowing of the initially broad isotope distributions which leads to an increase of the isoscaling coefficients α for cold fragments. The variation of α with γ is thus considerably reduced with the effect that the value $\alpha < 0.3$ measured for the most central bins can only be reproduced with input values $\gamma \leq 10 \text{ MeV}$. This is illustrated in Fig. 3, bottom right, which also shows the effect of possible variations of the isotopic composition of the two systems at breakup. Transport models predict that this difference should not change by more than a few percent [21].

4 Projectile fragmentation with ALADIN

In a very recent experiment with the ALADIN spectrometer, the possibility of using secondary beams for reaction studies at relativistic energies has been explored [22]. Beams of ^{107}Sn , ^{124}Sn , ^{124}La , and ^{197}Au were used to investigate the mass and isospin dependence of projectile fragmentation at 600 MeV per nucleon. The neutron-poor radioactive projectiles ^{107}Sn and ^{124}La were produced at the Fragment Separator FRS by fragmentation of a primary beam of ^{142}Nd and delivered to the ALADIN experiment. Natural Sn targets with areal density 500 mg/cm^2 were used in order to fully cover the rise and fall regimes of multifragmentation [19]. A cross sectional view of the experimental setup and a short description are given in the contribution of De Napoli et al. to this workshop [23].

The mass resolution obtained for projectile fragments entering into the acceptance of the spectrometer is about 1.5% for fragments with $Z \geq 6$ and increases up to about 3% for the lightest fragments. The error in the mass determination has about equal contributions from the measurement of the magnetic rigidity ($\Delta R/R \approx 1\%$) and from the time-of-flight measurement ($\Delta t \approx 150 \text{ ps}$, increasing up to 250 ps for light fragments). Masses are individually resolved for fragments with atomic number $Z \leq 10$. The elements are individually resolved over the full range of atomic numbers up to the projectile Z with a resolution of $\Delta Z \leq 0.2$ obtained with the TP-MUSIC IV detector [22, 23].

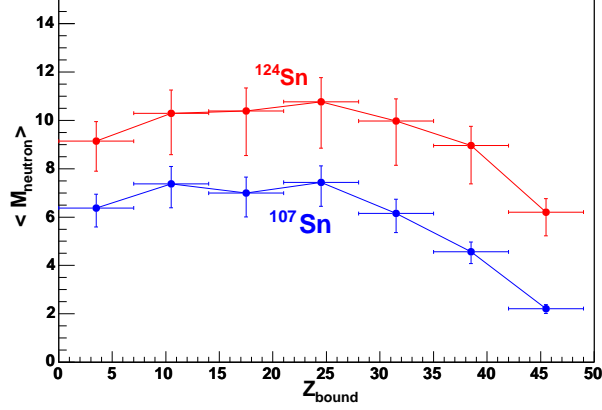


Figure 4: Neutron multiplicities of the spectator source for $^{107,124}\text{Sn}$ projectile fragmentation as a function of Z_{bound} (preliminary result).

Results of an analysis of the Z fluctuations of the largest fragment within a partition are presented in [23]. The preliminary analysis of isotope ratios obtained for the studied reactions shows that isoscaling is observed. The decrease of the isoscaling parameters with increasing centrality is confirmed and extended over the larger fragmentation regime covered in the collisions with the Sn target. If normalized to the larger difference in N/Z that is achieved by using radioactive beams the new data are found to be consistent with the results obtained for ^{12}C on $^{112,124}\text{Sn}$.

There is justified hope that the detection of projectile fragments without threshold with the ALADIN spectrometer will eventually permit the reconstruction of the spectator system at breakup. Fragments with $Z \geq 3$ exhibit well defined rapidity distributions centered near projectile rapidity [19]. It will be necessary, however, to also identify the spectator sources of hydrogen and helium ions and of neutrons.

Neutrons emitted in directions close to $\theta_{\text{lab}} = 0^\circ$, are detected with the Large-Area Neutron Detector (LAND) which covers about one half of the solid angle required for neutrons from the spectator decay. A preliminary analysis of the invariant multiplicity distributions of neutrons has led to the identification of the spectator sources of neutrons. They are characterized by temperatures up to about 4 MeV possibly caused by large contributions from evaporation. Reconstructed multiplicities for $^{107,124}\text{Sn}$ projectile fragmentation as a function of Z_{bound} are shown in Fig. 4. On average about 3 to 4 more neutrons are observed for the more neutron rich spectator system.

5 Conclusion

The present study of the role of the symmetry energy in spectator decay is motivated by the importance of this quantity for our understanding of astrophysical phenomena like supernovae and neutron stars. The similarity of the thermodynamic conditions reached in nuclear multifragmentation and in supernova explosions gives experimental access to properties of hot supernova matter and its nuclear composition. The observed reduction of the symmetry term coefficient needed to describe isotopic distributions is consistent with a global classification of multifragmentation as a low-density phenomenon. More specifically, it may indicate that small and intermediate-mass nuclei are produced which are surrounded by other fragments and by a nucleon gas. The structure of these highly excited fragments, at the chemical freeze-out point, may be considerably different from that of stable nuclei. The combined effects of the interaction with the neighbours and of their own expanded structure provide sufficient reason for a strong reduction of the symmetry term.

In order to draw firm conclusions the evolution of the spectator systems prior to breakup will have to be followed in more detail. The new experiments performed with the ALADIN spectrometer and with secondary beams offer the possibility to reconstruct the neutron-to-proton ratios of the systems at breakup. A spectator source of neutrons has been identified by analyzing the coincident data measured with LAND. The secondary decay of excited fragments has the effect of reducing the widths of the isotope distributions and of narrowing their overall separation in N/Z . Model calculations indicate that a reduction of the symmetry term will be partly masked by the sequential decay, with the effect that the true reduction at breakup may be considerably larger than what is observed for the final fragments.

The authors would like to thank T. Gaitanos for providing the results of RBUU calculations for the studied systems. C.Sf. acknowledges the receipt of an Alexander-von-Humboldt fellowship. This work was supported by the European Community under contracts No. ERBFMGECT950083 and RII3-CT-2004-506078 and by the Polish Scientific Research Committee under contract No. 2P03B11023.

References

- [1] J.M. Lattimer and M. Prakash, Phys. Rep. **333**, 121 (2000).
- [2] A.S. Botvina and I.N. Mishustin, Phys. Lett. B **584**, 233 (2004).

- [3] M. Baldo *et al.*, Nucl. Phys. **A736**, 241 (2004).
- [4] Bao-An Li, Phys. Rev. Lett. **88**, 192701 (2002).
- [5] V. Greco *et al.*, Phys. Lett. B **562**, 215 (2003).
- [6] Bao-An Li *et al.*, contribution to this workshop.
- [7] J.P. Bondorf *et al.*, Phys. Rep. **257**, 133 (1995).
- [8] A.S. Botvina, O.V. Lozhkin and W. Trautmann, Phys. Rev. C **65**, 044610 (2002).
- [9] A.S. Botvina and I.N. Mishustin, Phys. Rev. C **72**, 048801 (2005).
- [10] M.B. Tsang *et al.*, Phys. Rev. Lett. **86**, 5023 (2001).
- [11] G.A. Souliotis *et al.*, Phys. Rev. C **68**, 024605 (2003).
- [12] W.A. Friedman, Phys. Rev. C **69**, 031601(R) (2004).
- [13] M.B. Tsang *et al.*, Phys. Rev. C **64**, 054615 (2001).
- [14] A. Ono *et al.*, Phys. Rev. C **68**, 051601(R) (2003).
- [15] A.S. Botvina, A.S. Iljinov, and I.N. Mishustin, Sov. J. Nucl. Phys. **42**, 712 (1985).
- [16] L. Beaulieu *et al.*, Phys. Lett. B **463**, 159 (1999) and Phys. Rev. Lett. **84**, 5971 (2000).
- [17] A.S. Botvina and I.N. Mishustin, Phys. Rev. C **63**, 061601(R) (2001).
- [18] J. Pouthas *et al.*, Nucl. Instr. Meth. in Phys. Res. **A357**, 418 (1995).
- [19] A. Schüttauf *et al.*, Nucl. Phys. **A607**, 457 (1996).
- [20] A. Le Fèvre *et al.*, Phys. Rev. Lett. **94**, 162701 (2005).
- [21] T. Gaitanos *et al.*, Nucl. Phys. **A732**, 24 (2004), and private communication.
- [22] C. Sienti *et al.*, Nucl. Phys. **A749**, 83c (2005).
- [23] M. De Napoli *et al.*, contribution to this workshop.